

PDF hosted at the Radboud Repository of the Radboud University Nijmegen

The following full text is a publisher's version.

For additional information about this publication click this link.

<http://hdl.handle.net/2066/76594>

Please be advised that this information was generated on 2021-09-26 and may be subject to change.

Magnetic Resonance Studies on Porous Alumina doped with Iron and Chromium

Simion Simon,[†] André van der Pol, Ed J. Reijerse, Arno P. M. Kentgens, Geert-Jan M. P. van Moorsel and Engbert de Boer*

Department of Molecular Spectroscopy, Faculty of Science, University of Nijmegen, Toernooiveld, 6525 ED Nijmegen, The Netherlands

A combined magic-angle spinning (MAS) NMR and electron paramagnetic resonance (EPR) study has been performed on Fe- and Cr-doped alumina as a function of the heat-treatment temperature. Between 300 and 600 °C large quantities of tetra- and penta-coordinated Al were produced in porous xerogels. The penta-coordinated Al species have been found to be related to the catalytic activity. It has been found that the Fe ions accelerate the transition from γ - to α -Al₂O₃ and were mainly found within the alumina granules. On the other hand, Cr ions in high oxidation states (Cr⁵⁺, Cr⁶⁺) hampered the transition from γ - to α -Al₂O₃ and it has been proposed that they are preferentially situated on the surfaces of the granules.

Aluminas exist in a large variety of amorphous and microcrystalline forms with high surface areas that are widely used as catalysts or catalyst supports.¹ At high treatment temperatures they all transform into α -Al₂O₃ (corundum). The transition from γ - to α -Al₂O₃ dramatically reduces the surface area and, accordingly, the catalytic potency. It is therefore of interest to investigate the influence of small quantities of other oxides on the transition temperature from γ - to α -Al₂O₃. The stability of γ -Al₂O₃ at high temperature is very important in some applications, e.g. catalysts for automobile emission control.² It is already known that Fe³⁺ and Cr³⁺ affect the $\gamma \rightarrow \alpha$ transition,^{3,4} but understanding on a molecular level is lacking.

Paramagnetic doped alumina has been studied extensively by EPR,⁵⁻⁷ optical^{8,9} and diffuse reflectance spectroscopies.¹⁰⁻¹¹ The simultaneous use of EPR and NMR techniques for the investigation of doped alumina from starting solution up to stable α -Al₂O₃ is still unreported in the literature.

In this paper we present the results of a combined NMR and EPR investigation on Fe- and Cr-doped alumina as a function of the heat-treatment temperature. At heat-treatment temperatures between 300 and 600 °C large quantities of tetra- and penta-coordinated Al are produced in porous xerogels.¹² The penta-coordinated Al species are related to the catalytic activity.¹³ It is found that Fe ions accelerate the transition from γ - to α -Al₂O₃ and are mainly found in the interior of the alumina granules. On the other hand, Cr ions in high oxidation states hamper the transition from γ - to α -Al₂O₃ and it is proposed that they are preferentially situated on the surfaces of the granules. We focus particular attention on the stability of the γ -phase of alumina because it is involved in many catalytical applications.

Experimental

Alumina samples were prepared with the composition Al_{2(1-x)}M_{2x}O₃ with $x = 0$ and 0.002 and M = Fe, Cr. Although the synthesis has been described in detail in the literature,¹⁴ a short description of it is appropriate here. To a mixture of Al(NO₃)₃ · 9H₂O and M(NO₃)₃ · 9H₂O, 10 wt.% glycerol was added as reducing agent along with a small amount of water, so that clear solutions were obtained. Sub-

sequent heating of these solutions at 95 °C for 1.5 h resulted in viscous gels. Prolonged heating yielded spongy, bulky solid samples (xerogels). These solid samples were heated in the open air for 30 min at various temperatures, T_1 (°C). Immediately after heating, the samples were sealed in quartz EPR tubes or placed in airtight bottles for NMR measurements. Just before the beginning of the NMR measurements the samples were rapidly transferred to the spinners in order to minimize hydration effects. The samples are denoted by AM_x-T_y, where x refers to the fraction of M and y to the treatment temperature ($y = T_1/100$).

The crystalline phases obtained at high heat-treatment temperatures were identified by X-ray diffraction (XRD) at room temperature with a Philips PW 1820 X-ray powder diffractometer. ²⁷Al NMR measurements were carried out at room temperature on a Bruker AM-500 spectrometer. For the MAS NMR experiments a home-built probehead equipped with a Jakobsen 5 mm spinning assembly was used. Excitation pulses of 1 μ s and spinning speeds up to 14 kHz were typically employed. Spectra were referenced with respect to an external Al(NO₃)₃ solution [Al(H₂O)₆³⁺].

EPR spectra were recorded on a Bruker ESP-380 X-band spectrometer at room temperature for solid samples and at 140 K for sol and gel samples. The average microwave frequency was 9.3 GHz.

Results

X-Ray Measurements

All samples remained amorphous up to 700 °C. At higher temperatures, broad lines characteristic of γ -Al₂O₃ were first observed, followed by sharp lines belonging to α -Al₂O₃. The latter was the only phase present after heating for 30 min at 1200 °C. In Table 1 the observed phases have been summarized for the undoped and doped samples after 0.5 and 24 h heat treatment at 860 °C.

²⁷Al NMR

Fig. 1 shows ²⁷Al NMR spectra of alumina (AM₀-T_y) as a function of the heat-treatment temperature. The samples labelled sol and gel were measured without spinning. As expected, below 200 °C only one resonance was observed which was due to Al hexa-coordinated to water, hydroxy

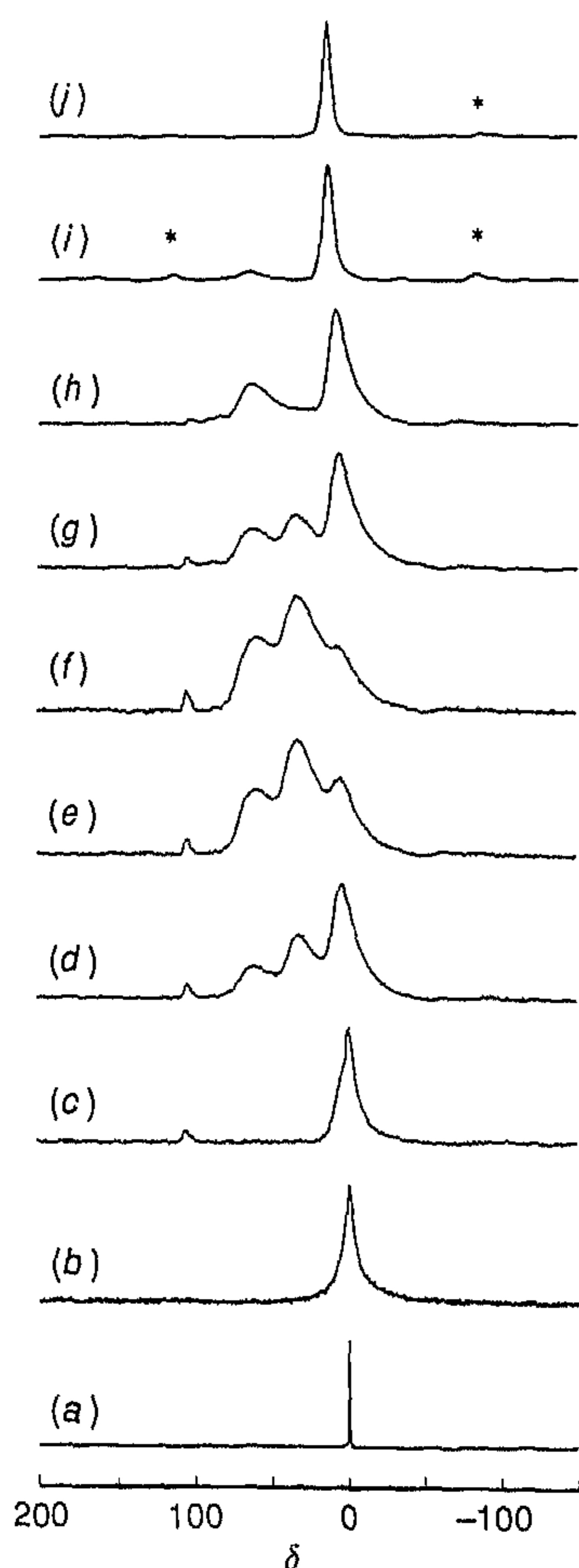
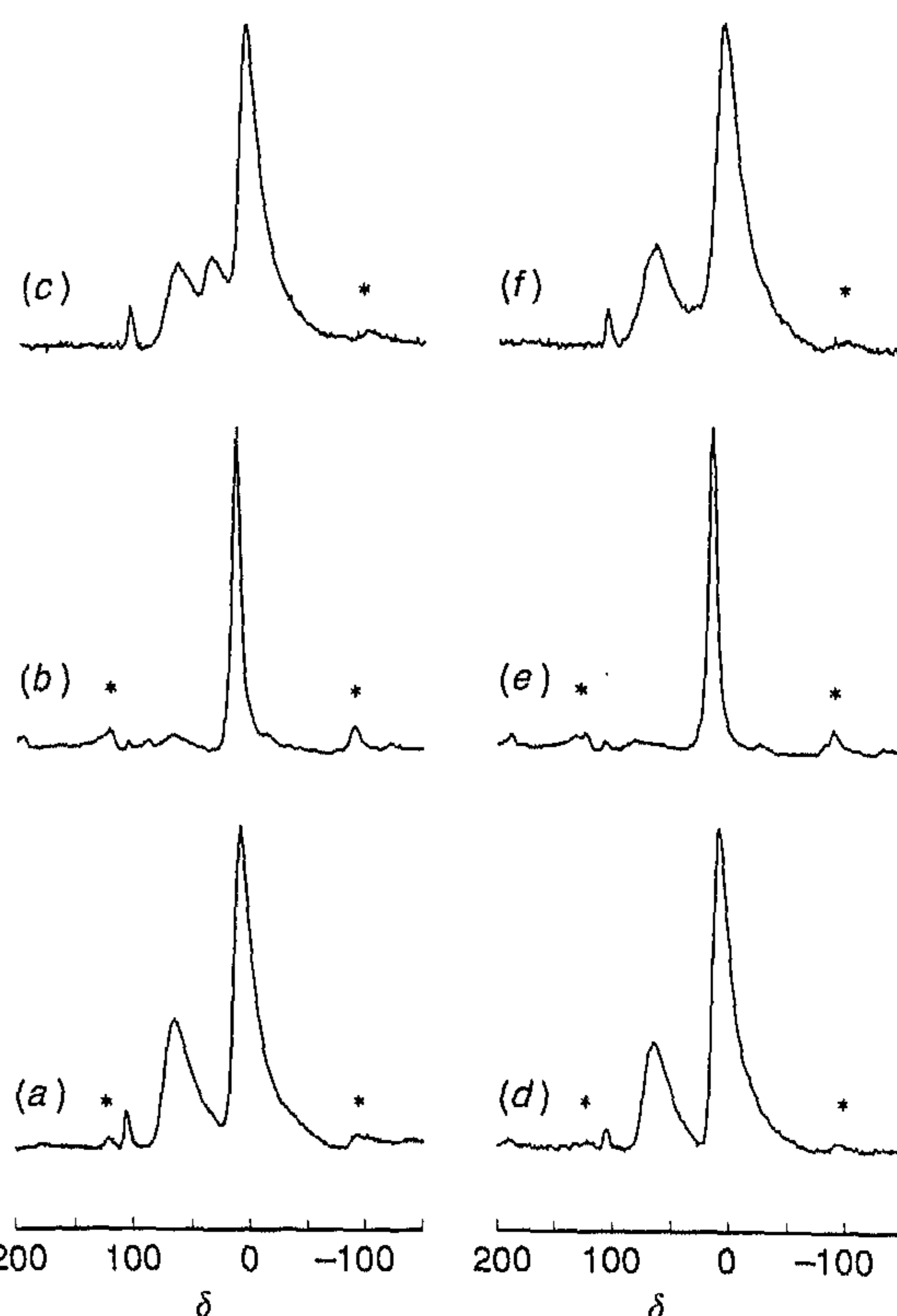
[†] Permanent address: Faculty of Physics, Babes-Bolyai University, 3400 Cluj-Napoca, Romania.

Table 1 Crystalline phases observed for undoped and doped samples after 0.5 and 24 h heat treatment at 860 °C

Heat-treatment time/h	sample		
	undoped (AM ₀ -T _{8.6})	iron-doped (AFe _{0.002} -T _{8.6})	chromium-doped (ACr _{0.002} -T _{8.6})
0.5	γ	α, γ	γ
24	γ	α	γ

groups or oxygen atoms. The linewidth of this resonance peak increases with increasing temperature as a result of network formation and accordingly decreasing mobility of the hexa-coordinated Al. At $T_i \geq 200$ °C three resonances developed in the ranges 0–8, 30–36 and 60–64 ppm, which were assigned previously to hexa-, penta- and tetra-coordinated Al, respectively.¹⁵

The small peak at *ca.* 105 ppm is from AlN, present as an impurity in the Si₃N₄ spinner. Between 200 and 300 °C rapid development of penta- and tetra-coordinated Al takes place almost simultaneously. Between 300 and 600 °C the fraction of penta-coordinated Al reaches its maximum value of *ca.* 0.5. Above 600 °C penta-coordinated Al gradually disappears until at 1200 °C only α-Al₂O₃ is present, containing hexa-coordinated Al.

**Fig. 1** ²⁷Al NMR spectra of undoped alumina samples showing the effect of heat-treatment temperature. (a) Sol, (b) gel, AM₀-T_γ with γ: (c) 1, (d) 2.5, (e) 3, (f) 6, (g) 7.5, (h) 8.6, (i) 10, (j) 12. All spectra were measured at room temperature and, except for sol and gel samples, with magic-angle spinning. Spinning side bands are indicated by *.**Fig. 2** ²⁷Al MAS NMR spectra of (a), (d) undoped (AM₀-T_{8.6}) and (b), (e) Fe- and (c), (f) Cr-doped samples (AM_{0.002}-T_{8.6}) after heat treatment at 860 °C for (a)–(c) 30 min and (d)–(f) 24 h. Spinning side bands are indicated by *.

In Fig. 2 the ²⁷Al MAS NMR spectra of undoped and doped samples, heated for 30 min [Fig. 2(a)] and 24 h [Fig. 2(b)] at 860 °C are presented. At this temperature the undoped sample, AM₀-T_{8.6}, consists of γ-Al₂O₃. The spectrum shows only resonances due to four- and six-coordinated Al in a ratio of 1 : 2.

Surprisingly, the presence of a small amount of iron and chromium strongly influences the thermal stability of the γ-phase. The presence of iron lowers the transition temperature from γ- to α-Al₂O₃, whereas chromium has the opposite effect. To be more specific, the small fraction of tetra-coordinated Al of the γ-phase in the undoped sample at 1000 °C [Fig. 1(i)] is already present in the Fe-doped sample treated at $T_i = 860$ °C. On the other hand, in the Cr-doped sample heated for 30 min at 860 °C, penta-coordinated Al can be distinguished, as is the case for the undoped samples treated at 750 °C. Even after 24 h of heating at 860 °C the NMR spectrum of the Cr-doped sample still shows features of distorted Al surroundings. Taking the AlN signal as an intensity indication, it can further be concluded that in the Cr-doped sample an appreciable fraction of Al is not detectable. This loss is probably due to the presence of paramagnetic ions¹⁶ and the severe line broadening of a number of highly distorted surface sites.¹⁷

EPR

Fe-doped Alumina

Fig. 3 shows the EPR spectra of the Fe-doped samples as a function of the heat-treatment temperature. Up to 750 °C the main feature is the signal at $g = 4.28$, which is typical for Fe³⁺ ($S = 5/2$) in disordered systems.¹⁸ The derivative linewidth decreases from 8 mT for the gel sample to 3 mT for the sample labelled T_{7.5}. A completely new spectrum develops at higher treatment temperatures at the expense of the signal at

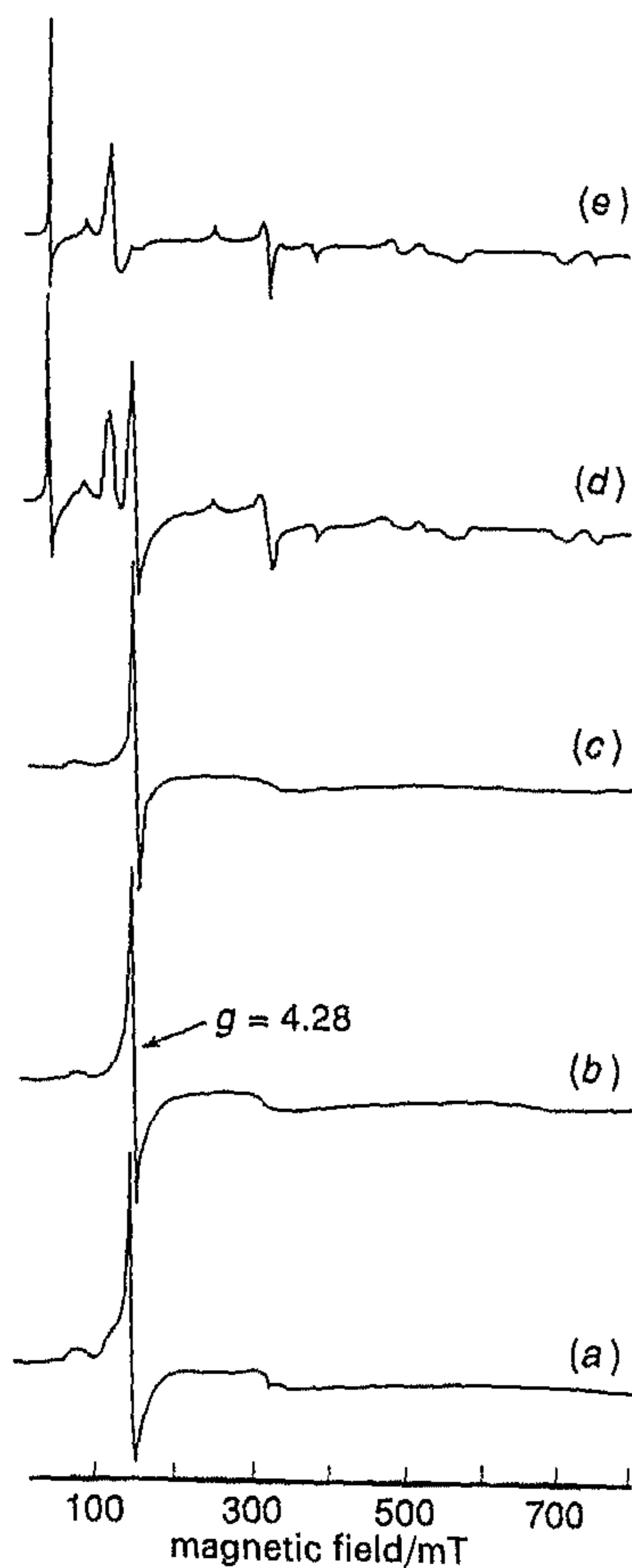


Fig. 3 EPR spectra of Fe-doped alumina as a function of heat-treatment temperature. (a) Gel, $\text{AlFe}_{0.002}\text{-T}_y$ with y : (b) 1, (c) 7.5, (d) 8.6 for 30 min, (e) 8.6 for 24 h. Spectrum (a) was measured at 140 K, other spectra at room temperature.

$g = 4.28$. For instance, after heat treatment for 30 min at 860°C , the temperature at which only $\gamma\text{-Al}_2\text{O}_3$ exists in the undoped sample, the new spectrum is already well developed. After 24 h heat treatment at 860°C the signal at $g = 4.28$ is absent and the remaining spectrum is identical to the well known powder spectrum of Fe-doped corundum.¹⁹ This means that in the Fe-doped sample we already have $\alpha\text{-Al}_2\text{O}_3$ at 860°C , in agreement with the X-ray and NMR results (Fig. 2).

Cr-doped Alumina

Fig. 4 illustrates the changes in the local environment and in the oxidation state of chromium upon heating the Cr-doped sample. The signal at $g = 1.97$ of the sol sample can be ascribed to Cr^{3+} ($S = 3/2$) hexa-coordinated to H_2O in a slightly distorted octahedral configuration.²⁰ A new spectrum is observed for the dry gel (T_1) with dominant lines at $g = 2.0$ and $g = 5.6$, apart from the small peak at $g = 4.28$ (see Fig. 4) which is due to Fe^{3+} present as an impurity in aluminium nitrate (*ca.* 0.03%). This new spectrum was assigned to Cr^{3+} ions subjected to a strong orthorhombic crystal field arising from a slightly distorted octahedral environment.²¹ The intermediate spectrum [Fig. 4(b)] is mainly a superposition of the sol and $\text{ACr}_{0.002}\text{-T}_1$ spectra. It is evident that in the viscous gel sample several Cr complexes are present with different six-coordinated geometries.

An important change in the spectra occurred at higher treatment temperatures. Between $T_1 = 100$ and 800°C a single, relatively narrow (derivative linewidth *ca.* 5 mT), symmetrical line was observed which is usually assigned to penta-coordinated Cr^{5+} ($S = 1/2$) ions.²² After 24 h treatment at 860°C a new spectrum developed (marked with asterisks) at

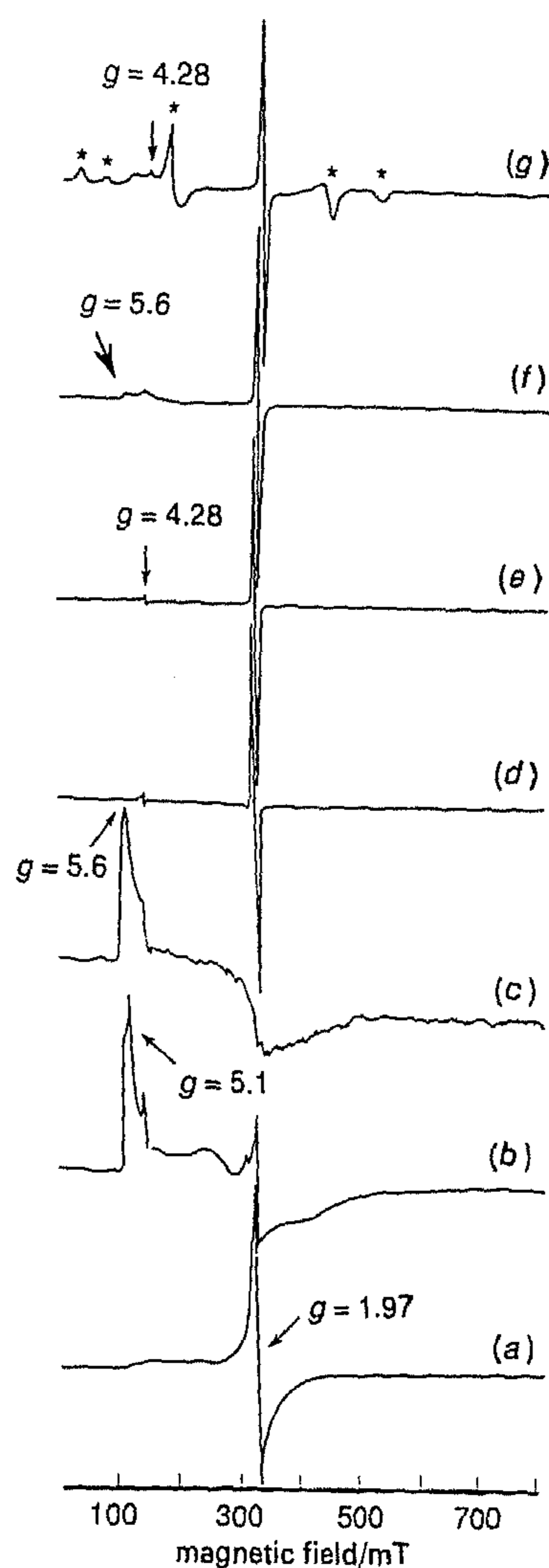


Fig. 4 EPR spectra of Cr-doped alumina as a function of heat-treatment temperature. (a) Sol, (b) gel, $\text{ACr}_{0.002}\text{-T}_y$ with y : (c) 1, (d) 2, (e) 7.5, (f) 8.6 for 30 min, (g) 8.6 for 24 h. Spectra (a) and (b) were measured at 140 K, other spectra at room temperature.

the expense of the narrow signal at $g = 1.97$. This spectrum was identical to the well known spectrum of ruby (Cr-doped corundum). This spectrum has been simulated with the zero field splitting parameters $D = 0.193 \text{ cm}^{-1}$ and $E = 0$.²³ Note that the strong line due to iron at *ca.* 50 mT in the spectrum of the Fe-doped sample $T_{8.6}$ is absent in the spectrum of the Cr-doped sample $T_{8.6}$.

Discussion

To understand the opposite effects of the Fe and Cr ions on the formation of xerogels and eventually on the formation of γ - and $\alpha\text{-Al}_2\text{O}_3$, we recall the molecular mechanisms occurring during the synthesis. In the starting solution small Al oligomers are produced by the interlinking of Al octahedra. The presence of water prevents extensive polymerization. During the drying and precipitation process these small oligomers agglomerate to form larger particles (granules) leading to viscous liquids and dry gels. At heating temperatures of *ca.* 200°C dehydroxylation and pyrolysis of glycerol commence and simultaneously low-coordinated Al species are formed. The maximum fraction of these species is observed for amorphous xerogels with $3 < y < 6$ and amounts to *ca.* 0.7.

Recently we showed that a considerable part of the low-coordinated Al is situated on the surfaces of the xerogels.¹² As shown here, the presence of Fe³⁺ and Cr³⁺ in the starting solutions have opposite effects on the formation of the xerogels and on the subsequent formation of γ - and α -Al₂O₃, despite the similar electronegativity and coordination number of Fe³⁺ and Cr³⁺. High-spin Fe³⁺ ($S = 5/2$) exhibits no crystal field stabilization in an octahedral environment. Therefore it will be easily available for incorporation into the Al oligomers by formation of M—OH—M bridges.²⁴ In contrast, high-spin Cr³⁺ ($S = 3/2$) is stabilized in an octahedral crystal field. This would imply a lower reactivity of Cr³⁺ towards such bridge formation. As a result of this, Cr³⁺ ions have a tendency to remain in solution. On continuing the heat treatment we therefore suggest that xerogels are produced with Fe³⁺ located mainly inside the xerogels and with Cr³⁺ located preferentially on the surfaces of the xerogels. This difference in behaviour of Fe³⁺ and Cr³⁺ during the synthesis is reflected in both the NMR and EPR spectra.

The Fe³⁺ ions inside the alumina xerogels act as sites for the formation of γ - and subsequently α -Al₂O₃. Fig. 2 shows that at $T_1 = 860^\circ\text{C}$ the Fe-doped sample is mainly in the α -phase, whereas the undoped sample is still in the γ -phase at this temperature. Thus Fe³⁺ ions accelerate the transformation from γ - to α -Al₂O₃. The EPR spectra of the Fe-doped sample shown in Fig. 3 support the conclusions drawn from NMR results. From the decrease in linewidth of the signal at $g = 4.28$ going from the gel to AFe_{0.002}-T_{7.5} it may be inferred that the changes in the environments of Fe³⁺ are minor. In Fig. 3(d) the line at $g = 4.28$ can still be observed and therefore the α -phase in addition to the γ -phase is present at $T_1 = 860^\circ\text{C}$. This is in agreement with XRD and NMR results. If the heat treatment procedure is extended to 24 h only the α -phase remains.

As mentioned above, the Cr-doped sample exhibits a different behaviour. The formation of the γ -phase is hampered compared with the undoped sample. The EPR spectra in Fig. 4 give information on the kind of Cr complexes present in the gels. When the gel is formed, in addition to the Cr³⁺ species giving rise to the signal at $g = 1.97$, there are Cr³⁺ complexes attached to the surfaces of the formed granules which are responsible for the signals at $g = 2.0$ and $g = 5.6$ [see Fig. 4(c)]. Between $T_1 = 100$ and 200°C only one signal is detected, which is generally ascribed to Cr⁵⁺ in a square-pyramidal configuration (*i.e.* penta-coordinated species).²² It is known that on heating Cr gels at 200°C higher oxidation states of chromium are generated (Cr⁵⁺ and Cr⁶⁺). The presence of an active oxidant like NO₃⁻ facilitates the oxidation,²⁵ so that below 200°C these high oxidation states are formed. In Fig. 4(f) a small peak at $g = 5.6$ (see arrow) can be discerned, which is definitely not present in the T_{7.5} spectrum [Fig. 4(e)]. From this it can be concluded that chromium is partly reduced to Cr³⁺. Prolonged heat treatment at 860°C for 24 h produces the spectrum of Cr³⁺-doped α -Al₂O₃. Note that a strong signal from Cr⁵⁺, a small peak at $g = 5.6$ from Cr³⁺ and a small signal from Fe³⁺ at $g = 4.28$ (see arrow) are still present. These facts can only be reconciled by the simultaneous presence of γ - and α -Al₂O₃. Note that the corresponding NMR spectrum and XRD pattern show only the presence of γ -Al₂O₃. A plausible explanation for this is that Cr³⁺ ions situated on the surface of the granules are in the α -phase, whereas in the inside of the granules the γ -phase still exists. This explanation is supported by the absence of an iron signal at *ca.* 50 mT, which should be easily detectable if Fe³⁺ were in α -Al₂O₃ (see Fig. 3). The lack of ²⁷Al MAS NMR signals due to α -Al₂O₃ may be caused by the relatively high concentration of paramagnetic Cr ions in

the small fraction of the α phase (too small to be detected by XRD), which will broaden the ²⁷Al resonances beyond detection.

Conclusions

Porous amorphous alumina with a high fraction of penta-coordinated Al can be prepared by decomposition of aluminium nitrate solutions associated with glycerol oxidation. A fraction of the low-coordinated Al species were found on the surfaces of the xerogels.

In alumina samples doped with Fe³⁺ or Cr³⁺ ($x = 0.002$), low-coordinated Al species were also formed. Iron accelerated the transition from γ - to α -Al₂O₃, whereas chromium hampered not only this transition, but also the formation of γ -Al₂O₃. Furthermore, Fe³⁺ ions were mainly situated within the alumina granules whilst Cr³⁺ ions were preferentially located on the surface of the granules.

The authors thank J. M. M. Smits for XRD measurements and A. A. K. Klaassen, G. E. Janssen and Mrs G. H. Nachtegaal for their technical assistance.

References

- 1 H. Knözinger and P. Ratnasamy, *Catal. Rev. Sci. Eng.*, 1978, **17**, 31.
- 2 P. Burtin, J. P. Brunelle, M. Pijolat and M. Soustelle, *Appl. Catal.*, 1987, **34**, 225.
- 3 G. C. Bye and G. T. Simpkin, *J. Am. Ceram. Soc.*, 1974, **57**, 367.
- 4 T. Tsuchida, R. Furuichi, T. Ishii and K. Itoh, *Thermochim. Acta*, 1983, **64**, 337.
- 5 C. J. Carman and W. J. Kroenke, *J. Phys. Chem.*, 1968, **72**, 2562.
- 6 A. Ellison and K. S. W. Sing, *J. Chem. Soc., Faraday Trans. 1*, 1978, **74**, 2807.
- 7 A. S. Hare and J. C. Vickerman, *J. Chem. Soc., Faraday Trans. 1*, 1981, **77**, 1103.
- 8 Y. Hirai, T. Fukuda, Y. Kobayashi, H. Kuwahara, Y. Kido and K. Kubota, *Solid State Commun.*, 1987, **62**, 637.
- 9 G. Carturan, R. DiMaggio, M. Montagna, O. Pilla and P. Scardi, *J. Mat. Sci.*, 1990, **25**, 2705.
- 10 B. M. Weckhuysen, L. M. de Ridder and R. A. Schoonheydt, *J. Phys. Chem.*, 1993, **97**, 4756.
- 11 B. M. Weckhuysen, A. A. Verbeckmoes, A. L. Buttiens and R. A. Schoonheydt, *J. Phys. Chem.*, 1994, **98**, 579.
- 12 S. Simon, A. van der Pol, E. J. Reijerse, A. P. M. Kentgens, G. J. M. P. van Moorsel and E. de Boer, *J. Chem. Soc., Faraday Trans.*, 1994, **90**, 2663.
- 13 F. R. Chen, J. G. Davis and J. J. Fripiat, *J. Catal.*, 1992, **133**, 263.
- 14 F. Abbatista, A. Delmastro, G. Gozzelino, D. Mazza, M. Vallino, G. Busca and V. Lorenzelli, *J. Chem. Soc., Faraday Trans.*, 1990, **86**, 3653.
- 15 M. E. Smith, *Appl. Magn. Reson.*, 1993, **4**, 1.
- 16 A. P. M. Kentgens, A. Bos and P. J. Dirken, *Solid State Nucl. Magn. Reson.*, 1994, **3**, 315.
- 17 B. A. Huggins and P. D. Ellis, *J. Am. Chem. Soc.*, 1992, **114**, 2098.
- 18 D. L. Griscom, *J. Non-Cryst. Solids*, 1980, **40**, 211.
- 19 J. van Dijk, Ph.D. Thesis, Technical University Delft, 1976.
- 20 R. Karthein, H. Motschi, A. Schweiger, S. Ibric, B. Sulzberger and W. Stumm, *Inorg. Chem.*, 1991, **30**, 1606.
- 21 S. Doeuff, M. Henry, C. Sanchez and J. Livage, *J. Non-Cryst. Solids*, 1987, **89**, 84.
- 22 D. Cordischi, M. Cristina Campa, V. Indovina and M. Occhiuzzi, *J. Chem. Soc., Faraday Trans.*, 1994, **90**, 207.
- 23 D. E. O'Reilly and D. S. MacIver, *J. Phys. Chem.*, 1962, **66**, 276.
- 24 J. Livage, M. Henry and C. Sanchez, *Prog. Solid State Chem.*, 1988, **18**, 259.
- 25 N. E. Fouad, H. Knözinger, M. I. Zaki and S. A. A. Mansour, *Z. Phys. Chem.*, 1991, **171**, 75.